Combining conventional tree-ring measurements with wood anatomy and strontium isotope analyses enables dendroprovenancing at the local scale

COMBINING CONVENTIONAL TREE-RING MEASUREMENTS WITH WOOD ANATOMY AND STRONTIUM ISOTOPE ANALYSES ENABLES DENDROPROVENANCING AT THE LOCAL SCALE

D'Andrea R.,[1] Corona C.,[2-3-4] Poszwa A.,[5] Belingard C.,[1] Domínguez-Delmás M.,[6] Stoffel M.,[3-4-7] Crivellaro A.,[8-9] Crouzevialle R.,[1] Cerbelaud F.,[1] Costa G.,[10] Paradis-Grenouillet S.[1-9]

[1] GEOLAB, Université de Limoges (Limoges, France)

[2] GEOLAB, UMR 6042 CNRS, Université Clermont Auvergne (Clermont-Ferrand, France)

[3] Climate Change Impacts and Risks in the Anthropocene, Institute for Environmental Sciences, University of Geneva (Geneva, Switzerland)

[4] Department F.A. Forel for Environmental and Aquatic Sciences, University of Geneva (Geneva, Switzerland)

[5] Laboratoire Interdisciplinaire des Environnements Continentaux, Université de Lorraine (Nancy, France)

[6] Amsterdam School for Heritage and Memory Studies, University of Amsterdam (Amsterdam, The Netherlands)

[7] Department of Earth Sciences, University of Geneva (Geneva, Switzerland)

[8] Forest Biometrics Laboratory, Faculty of Forestry, University of Suceava (Suceava, Ukraine)

[9] Éveha, Bureau d'étude archéologique (Limoges, France)

[10] Laboratoire PEIRENE, Université de Limoges (Limoges, France)

CORRESPONDING AUTHOR

Roberta D'Andrea
roberta.dandrea@etu.unilim.fr
33 rue François Mitterrand – 87032 Limoges (France)

ABSTRACT

Dendroprovenancing provides critical information regarding the origin of wood, allowing further insights into economic exploitation strategies and source regions of timber products. Traditionally, dendroprovenancing relies on pattern-matching of tree rings, but its spatial resolution is limited by the geographical coverage of species-specific chronologies available for crossdating and, in the case of short-distance trades, by scarce environmental variability. Here, we present an approach to provenance timber with high spatial resolution from forested areas that have been exploited intensively throughout history, with the aim to understand the sustainability of the various woodland management practices used to supply timber products. To this end, we combined tree-ring width (TRW), wood anatomical and geochemical analyses in addition to multivariate statistical validation procedures to trace the origin of living oak trees (*Quercus robur*) sampled in four stands located within a 30-km radius around the city of Limoges (Haute-Vienne, France). We demonstrate that TRW and wood anatomical variables (and in particular cell density) robustly discriminate the eastern from the western site, while failing to trace the origin of trees from the northern and southern sites. Here, strontium isotopic ratios ($^{87}Sr/^{86}Sr$) and Ca concentrations identify clusters of trees which could not be identified with TRW or wood anatomy. Ultimately, our study demonstrates that the coupling of wood anatomy with geochemical signatures allows to correctly pinpoint the origin of trees. Given the small geographic scale of our study and the limited differences in elevation and

climate between study sites, our results are particularly promising for future dendroprovenancing studies. We thus conclude that the combination of multiple approaches will not only increase the accuracy of dendroprovenancing studies at local scales, but could also be implemented at much larger scales to identify trends in historic timber supply throughout Europe.

KEYWORDS

Tree rings, *Quercus robur*, xylem anatomical traits, $^{87}Sr/^{86}Sr$, multi-proxy approach.

1. INTRODUCTION

Determining the geographic provenance of timber is paramount in fields of research dealing with both modern wood (e.g. conservation and biodiversity studies; forensic sciences fighting illegal logging; wine barrel industry) and wood from (pre)historical contexts (e.g. history, archaeology, art history, paleoecology/climatology). The identification of the geographic source of timber (i.e. dendroprovenancing; Eckstein and Wrobel, 2007) has provided insights into the use of local and far afield wood resources in different periods and places, and by inference, into the organization of timber supply and trade networks in the past (Domínguez-Delmás et al., 2014; Bernabei et al., 2019; Daly et al. 2021; Daly and Tyers, 2022). Dendroprovenancing is also used to identify source areas of historic wood used to reconstruct past climate variability (Büntgen et al., 2011; Cook et al., 2015), and to assist in the detection of illegally logged wood and illicit trafficking of art objects (Dormott et al., 2015; Gori et al., 2015; Crivellaro and Ruffinatto, 2020).

Scientific techniques used to determine the provenance of wood include visual, genetic and chemical methods (Dormontt et al., 2015). For example, species identification based on visual (i.e. observation of macro- and micro-wood anatomical features; Schoch et al., 2004; Gasson et al., 2011; Crivellaro et al., 2013; Ruffinatto and Crivellaro 2019) or chemical (i.e. analysis of biochemical compounds in wood; Coté, 1968; Hao et al, 2021) approaches can point towards the geographic provenance of species with restricted distribution areas (e.g. Traoré et al., 2018). DNA markers and haplotype determination have likewise been tested to pinpoint the origin of wood with different degrees of success on oak timbers from historic shipwrecks and buildings (Speirs et al., 2009; Akhmetzyanov et al., 2020a), modern oak used by the cooperage industry in France (Deguilloux et al., 2004), and on tropical species traded for furniture and other uses (Lowe and Cross, 2011; Paredes-Villanueva et al., 2019). Similarly, chemical techniques have been employed to analyze stable isotopes in wood to trace its origin. In fact, stable isotope ratios of carbon, oxygen and hydrogen measured in tree-ring cellulose will provide prime insights into the eco-physiological processes and related climate conditions governing tree growth at a given site (McCarroll and Loader, 2004). This information will be stored in the wood of growth rings and keep a specific isotopic fingerprint corresponding to the climatic factors from the site at which the tree grows, thereby tracing its provenance. Stable carbon isotopes, for instance, have provided good results in dry

areas of the Southwestern U.S. (Kagawa and Leavitt, 2010). In the same region, strontium isotopes were also used to pinpoint the provenance of ancient wood from Chaco Canyon (English et al., 2001; Reynolds et al., 2005). Unlike ratios of carbon, oxygen or hydrogen isotope, strontium isotopes are more independent of climatological conditions and can therefore provide a geochemical signature related to the soil in which trees grow (Hajj et al, 2017), which characteristics are linked to weathered rocks underneath. Strontium isotopes have also been used to trace the origin of historic wood in the Eastern Mediterranean (Rich et al., 2016a; 2016b), demonstrating that they are a good proxy for timber provenancing when the material has not been waterlogged (Hajj et al., 2017; Domínguez-Delmás et al., 2020b; Van Ham-Meert et al., 2020).

The oldest and most conventional approach employed to determine the provenance of (pre)historic wood originating from temperate forests is dendrochronology, the scientific discipline studying growth rings in wood to determine their age and provenance. In fact, annual alterations in environmental conditions induce year-to-year changes in the growth of tree rings (Fritts, 1976; Schweingruber, 1996), resulting in growth patterns (i.e. tree-ring series) that are characteristic for the tree species in a specific area. Differences in environmental conditions along the longitudinal, latitudinal and elevation gradients will induce spatial variations in growth patterns, allowing inferences about the source area of wood (Bridge, 2012). The most commonly used approach to provenance wood with tree rings consists in correlating the tree-ring series of the wood under study with site or regional ring-width chronologies (Baillie, 1982). The area represented by the reference chronology providing the strongest statistical match (using Student's *t*-value and/or Pearson's correlation coefficient) is then considered the potential source area of the wood. The approach to dendroprovenancing based on correlations assumes that the (dis-)similarity of tree growth can be quantified by statistical measures of proximity, and that statistical similarity means geographic vicinity (Gut, 2018). Yet, these assumptions have several pitfalls (Bridge, 2012; Gut, 2018), some of which have been addressed in recent studies (Fowler and Bridge, 2015; Drake, 2018; Gut, 2020). Furthermore, in climate regimes with low topographic complexity (e.g. climate of the Atlantic region), complacent tree growth is a major limiting factor for tree-ring based dendroprovenancing (Bridge, 2012; Drake, 2018; Domínguez-Delmás et al., 2020a; Gut, 2020). In studies focusing on short-distance timber trade (<100 km), these limitations are even more restrictive as the probability to find locally characteristic ring-width patterns decreases with shorter distances.

Novel analytical techniques have been developed in tree-ring research over the last decade. Among these, quantitative wood anatomy (QWA) is thought to have the largest potential to overcome some of the above caveats and to increase the robustness and precision of dendroprovenancing. In fact, QWA assesses variability of wood cell anatomical features in dated tree-rings (von Arx et al., 2016; Pritzkov et al., 2016; Souto-Herrero et al., 2017) and thus provides key insights into wood functional responses or growth conditions at intra-annual resolution. Such differences in anatomical features within annual growth rings does not only allow establishing past and current intra-annual structure-function relationships in trees, but also assessment of their sensitivity to environmental variability (e.g. Fonti and García-González, 2008; Zweifel et al. 2006; Eilmann et al. 2011). Series of wood anatomical features thus carry specific environmental signals prevailing at a given site at specific times of the growing season. As such, they contain signals which will not necessarily be replicated in the patterns encoded in ring-width series, thereby adding a key source of additional site - and species-specific information (Fonti and García-González, 2008; Campelo et al., 2010; Castagneri et al., 2015; Ziaco et al., 2016). These wood anatomical features therefore hold great potential to clarify and expand the environmental information contained in wood (Ziaco and Liang, 2019), and consequently to increase the accuracy of dendroprovenancing.

Enhancing the accuracy and resolution of wood provenance is paramount in studies dealing with domestic timber supply and historical forestry practices, as well as in multi-scale analyses of human-environment interactions that reach far into the past using historic timbers (Eissing and Dittmar, 2011; Gut, 2018; Muigg and Tegel, 2020; Tegel et al., 2022). Indeed, several authors pleaded for the use of a multi-proxy approach to further improve the accuracy of wood provenancing, namely in studies aimed at inferring the provenance of shipwreck timbers (Domínguez-Delmás et al., 2020b; Akhmetzyanov et al., 2020a; Akhmetzyanov et al. 2020b) or at pinpointing the origin of oak timbers in Northern Spain (Akhmetzyanov et al., 2019).

Here, we assess the potential of a multiproxy approach in which we combine tree-ring widths, quantitative wood anatomy and strontium isotopes from living oak (*Quercus robur* L.) trees to discriminate wood from four woodlands located around the city of Limoges (Haute-Vienne, France). The sites sampled likely supplied timber for construction activities in the city throughout the past millennium. We chose to focus our study on *Quercus*

robur as a vast majority of historic buildings in Limoges are made of oak wood. The small geographic scale of our study area (<100 km radius) makes this explorative study particularly challenging given the fairly limited geologic, topographic, and climatic variability within the region. At the same time, if successful, this study would clearly enhance the significance of its results beyond the regional character. In other words, the development of an approach allowing high-resolution provenancing of historically forested areas would push timber analyses to new frontier and would allow comparative studies about the success and failure of historical forestry practices towards sustainable timber production across different geographic regions.

2. MATERIALS AND METHODS

2.1 STUDY AREA AND SAMPLING SITES

This study was realized in the Haute-Vienne department of central France (Fig. 1a). Unlike coastal areas of continental Europe that have been deforested during the late Middle Ages and where timber provenance studies consequently have to address long-distance trade, the Nouvelle-Aquitaine region remained largely covered by broadleaf woodlands (Paradis-Grenouillet and Crouzevialle 2021). Wood drifting was thus limited to the rivers Taurion and Vienne, and it is attested from the 12th to the 19th centuries. Archival documents mention that forests located *c.* 30 km north and east of Limoges were intensively exploited to provide the city and the surrounding villages with firewood. Oak (*Quercus robur* and *Q. petraea*) timber employed in construction is never directly mentioned in the historical sources related to wood drifting, but it is reasonable to hypothesize that it was also collected from local forests and transported on the rivers (Paradis-Grenouillet and Crouzevialle 2021).

Within the study area, the sampling sites were chosen based on their potential to have supplied the city of Limoges with oak construction timber. Because archival documents referring to the transportation of oak timber products in Limoges do not contain any specific information on construction timber, we defined four areas of possible interest along the cardinal directions within a 30-km radius around Limoges. In each area, sites were identified according to three main criteria: (1) the age of oak trees (>50 yr) to maximize the chances to obtain robust, multi-decadal TRW and QWA chronologies; (2) limited micro-topography (i.e. relatively flat

areas) to avoid the occurrence of growth disturbances that are induced by factors other than climatic and would blur the climate signals in the tree-ring series; (3) comparable density and diameters of oak trees. To meet these criteria,–we analyzed times series of historical maps and aerial photographs (available at https://geoportail.gouv.fr) for a preliminary identification of private or public lots with a stable forest cover over the last three centuries. Although we initially considered limited anthropogenic disturbances as an additional, fourth selection criterion, we finally had to include in the site selection woodlands managed through the coppice-with-standards practice, as this was widespread in the region since ancient times. Four sites around Limoges met the above-mentioned criteria and were thus selected for analysis: Saint-Hilaire-les-Places (HIL), Bujaleuf (BUJ), Rochechouart (ROC), and Compreignac (COM). The characteristics and locations of the sites are provided in Fig. 1b and Table 1.

All stands are characterized by a predominance of pedunculate oaks (*Quercus robur L.*) mixed with sweet chestnuts (*Castanea sativa* Mill.) and European beech trees (*Fagus sylvatica* L.) and a limited elevational gradient ranging from 260 (ROC) to 430 m a.s.l. (COM). According to the 0.1 × 0.1 lat/long E-OBS gridded climate dataset (Cornes et al., 2018), mean annual temperatures (1950-2020) range between 10.65°C (BUJ) and 11.58°C (ROC). Precipitation totals average 914, 994, 1010, and 1078 mm at ROC, COM, HIL and BUJ, respectively. Temperature and precipitation conditions are characteristic of oceanic climate and are comparable among the four sites (Fig. 1c) with cool summers (15.5°C on average in June, July and August), mild winters (4°C in December, January and February) and the absence of a pronounced dry season. From a geological perspective, the substratum is composed primarily of plutonic rocks at all four sites, sometimes slightly metamorphized, on which more or less acidic soils of varying depth and fragmented rock content (depending on topographic context) have developed from granitic arenas (Table 2).

2.2 SAMPLE COLLECTION AND PREPARATION

At each site, 20 to 30 dominant pedunculate oak (*Quercus robur* L.) trees were sampled in October 2020 and in April 2021 based on their stem diameter and estimated age. For each tree, two 5.5 mm cores were extracted at breast height (*c.* 130 cm above ground) using a Pressler increment borer. At each site, five cores from five different trees were isolated and stored for geochemical analyses. All other samples were prepared using

131 standard dendrochronological procedures (Bräker, 2002): cores were air dried, glued onto wooden supports
132 and sanded using progressively finer sandpaper (i.e. 120, 240, 400 and 600 grit) before they were scanned at
133 2400 DPI using an Epson 10000 XL Scanner.

134 For wood anatomical measurements, we retained samples from those 10 trees showing the highest intra-site
135 correlations (see cross-dating procedure, section 3.2) at each site. Sanding dust was removed from vessel
136 lumina with a high-pressure air hose and cores were blackened with a permanent marker. Thereafter, vessels
137 were filled with pulverized white chalk to enhance contrast between the black ink and the white vessels for a
138 better quantification of vessel lumina. A series of high-resolution overlapping images of the tainted cores were
139 then acquired with an ATRICS device (ADVANCE system; Levanič, 2007). The resulting high-resolution Images
140 (i.e. four to seven depending on core length) were subsequently stitched together using Image Composite
141 Editor (https://www.microsoft.com/en-us/research/product/computational-photography-applications/image-
142 composite-editor/).

143 For each core previously stored for geochemical analyses, a 2g fragment of heartwood was cut and finely
144 ground manually. The next steps were done in a clean room in order to avoid any contamination.
145 Approximatively 200 mg of wood chips of each sample were placed in a glass tube previously washed. Samples
146 were suspended in ultrapure H_2O_2 for one night, then in ultra-pure nitric acid (69% Seastar) and mineralized
147 using a microwave digester (UltraWave Milestone). The resulting solutions were diluted to 10 ml with ultrapure
148 water.

149 ## 2.3 Development of tree-ring and wood anatomical chronologies

150 Overall TRW as well as early- (EW) and latewood (LW) widths were measured and cross-dated using the
151 CooRecorder / CDendro 7.6 software (Cybis 2016, http://www.cybis.se/forfun/dendro/index.htm). The ring-
152 porous structure of oak allowed for a clear distinction between EW and LW. Cross-dated series from the same
153 trees were averaged into individual TRW, EW and LW series. To remove age trends and trends related to forest
154 dynamics, series were detrended with a cubic smoothing spline (Cook et al., 1981) with a frequency response
155 of 50% at a wavelength of 30 years.

Vessel size parameters were measured semi-automatically on the stitched images using the ROXAS software (Von Arx and Carrer, 2014). Because most of the climate signal appears to be recorded by the largest vessels (García-González et al., 2016), vessels smaller than 10.000 μm^2 – typically formed in the late growing season – were excluded from further analyses. In total, we developed chronologies for ten vessel-related variables available from ROXAS outputs, which are mean cell lumen area (MLA), maximum cell lumen area (MaxLA), minimum cell lumen area (MinLA), number of cells (CNo), cumulative area of all counted cells (CTA), mean percentage of conductive area within xylem (RCTA), cell density (CD), theoretical hydraulic conductivity (Kh), theoretical xylem-specific hydraulic conductivity per annual ring (Ks), and mean hydraulic diameter per ring (Dh) (Table 3). Similar detrending procedures were used for the vessel, TRW, EW and LW chronologies (García-González et al., 2016). Statistics were computed for all detrended series using the *dplR* package (Bunn, 2008) in R 4.1.1 (R Core Team, 2020). These included mean inter-series correlation (Rbar), expressed population signal (EPS; Bunn, 2008) and first-order autocorrelation (AC). Running Rbar and EPS values were computed at each site using a 30-year moving window with a 29-year overlap to illustrate changes in the strength of common patterns of radial growth over time. We used an EPS≥0.85 threshold to attest the robustness of all site chronologies (Wigley et al., 1984; Buras, 2017).

2.4 Spatial patterns of time series and gradient analyses

Many of the 13 measured or derived variables (TRW, vessel variables) are correlated and carry redundant information (García-González et al., 2016; Akhmetzyanov et al., 2019). Therefore, we reduced the dimensionality of our dataset of interrelated site-series detrended chronologies with a principal component analysis (varimax-rotated PCA) and kept only those variables carrying the most complementary information based on their loadings on the first two principal components (González-González et al., 2016; Kniesel et al., 2015; García-González et al., 2016). To assess geographic patterns of annual variation in the PCA-selected proxies, we performed a Principal Component Gradient Analysis (PCGA; Buras et al., 2016) designed to identify clusters of shared growth patterns at the scale of individual trees and to visualize whether these clusters are related to available explanatory variables such as site or climatic parameters (Akhmetzyanov et al., 2020). The

PCGA makes use of polar coordinates of loadings from the first two axes obtained from a regular PCA to define tree-ring series of similar trends (Buras et al., 2016), thus allowing for a precise understanding of mechanisms causing population gradients. To test whether the PCGA-loadings indicate site specific growth signals, we applied a Wilcoxon rank-sum test which, when significant, indicates a difference in the non-parametric means between the PCGA loadings of site pairs.

In dendroprovenancing studies, the precise origin of timber is most of the time unknown. To test the legitimacy of the PCGA approach to pinpoint the origin of a tree, and hence evaluate its interest for dendroprovenancing, we sequentially removed one tree from our original dataset and recomputed the PCGA. To evaluate the geographic origin in the PCGA from this leave-one-out analysis, we (1) correlated the time series that was not included in the PCGA with the first two PCs and used the latter correlation values as PC loadings (Akhmetzyanov et al., 2019). For each site, we (2) averaged the Euclidean distances calculated between the PC-loadings of the left-out tree and the PC-loadings of each tree included in the PCGA. Lastly, (3) we assigned each left-out tree to a site based on the minimum mean Euclidean distance and computed a confusion matrix to assess the robustness of the PCGA for each TRW and vessel parameter.

2.5 Possible climatic drivers of the PCGA gradients

We then explored whether climatic variables could explain possible gradients detected during the PCGA. To this end, we performed correlation analyses between the detrended TRW and vessel chronologies and monthly climatic variables (1951-2020) using bootstrapped correlation functions (BCF) from the Treeclim package (Zang and Biondi, 2015) in R (R Core Team, 2016). In BCF, correlation of precipitation - considered as primary variable – with tree-growth was computed as a Pearson ’s linear correlation coefficient. This linear correlation was then removed to compute the partial correlation of the secondary variable (monthly temperature in our case) with the predictand.

Following the approach developed by Akhmetzyanov et al. (2019), we then correlated climatic variables identified as significant from the BCF with each tree-ring series using Spearman's rank correlation so as to account for non-normally distributed data. We used (1) the Spearman's rank correlation performed between

climate correlations and the PCGA rank to detect potential variations of climate correlations along the PCGA gradient and (2) the Wilcoxon rank-sum tests to highlight potential effects of geographic origin on climate correlations. Meteorological data included both monthly temperature and precipitation series extracted at each site from the E-OBS gridded dataset (0.1 × 0.1 lat/long, Cornes et al., 2018) and monthly standardized precipitation-evapotranspiration index (SPEI, 0.5 × 0.5 lat/long, Vicente-Serrano et al., 2012).

2.6 Major and trace element concentration analysis and $^{87}Sr/^{86}Sr$ ratios measurements in wood

Geochemical analysis (major and trace element concentration analysis and $^{87}Sr/^{86}Sr$ ratios measurements) were performed at SARM (CRPG Nancy). Aliquots of each sample were analyzed for major (ICP-OES Icp 6500 radial, Thermo-Scientific) and trace (ICP-MS Icap-Q, Thermo-Scientific) element concentration. In order to purify the solution and isolate the Sr from the rest of the matrix before isotopes measurements, the remaining solutions were evaporated in Teflon vials (Savillex) and the dry residues were recovered in ultrapure 2M HNO3 then passed through an ion exchange column (Pin et al, 1997). Sr isotope ratios were measured by Thermal Ionization Mass Spectrometry (TIMS Triton +, Thermo-Scientific). Samples were loaded (about 100ng of Sr) on a rhenium filament using 1 µl of a mixture of TaO2, HF and H3PO4 as activator. Analysis was performed with 5 blocks of 15 cycles. The isotopic ratios measured were corrected for the fractionation process in the mass spectrometer using normalization to the $^{88}Sr/^{86}Sr$ ratio of 8.375209 and ^{87}Sr was corrected for ^{87}Rb by measuring ^{85}Rb. During mass- spectrometer analysis, blank samples and control samples were routinely analyzed to check the quality of the upstream chromatographic separation. An international standard solution (NBS987) was analyzed during each set of measures to monitor and correct the isotopic ratios of the sample. For each analysis day, the standard error (2SE) was determined from reproducibility of NBS 987 standard $^{87}Sr/^{86}Sr$ measurements. Values of 2SE varied between $8 * 10^{-6}$ to $1*10^{-5}$.

3 Results

3.1 Selection of variables

The principal component analyses performed at the four sites (39 trees in total over the period 1951-2020) on the spline-detrended chronologies allowed identification of similar clusters across all sites, with variables referring to radial growth (TRW, LW), to vessel size (MLA, MaxLA, Dh and Kh) and number of vessels (CNo and CD) (Fig. S1). As TRW, CD and MLA showed the highest contributions to PC1 and PC2 at all sites amongst the 13 ring-width and vessel chronologies available from tree-ring and wood anatomical analyses, they were retained for further analysis. Based on the PCA results, these variables belong to different clusters and are supposed to carry contrasting and site-specific information.

Higher Rbar, EPS and AC statistics were computed for TRW as compared to CD and MLA chronologies (Table 4). Despite the rather limited number of trees included in the four site chronologies, moving EPS, computed for TRW chronologies, exceeded the 0.85 threshold at all sites for most of the period 1951-2020 (Fig. 2). By contrast, CD and MLA chronologies failed to pass this threshold (Figs. S2, S3). The highest Rbar values were obtained for the TRW and CD series from Compreignac whereas comparable, albeit slightly lower, values are found at Bujaleuf, Saint-Hilaire-les-Places and Rochechouart. By contrast, for MLA, mean inter-series correlation was weaker at Compreignac (0.10) and Rochechouart (0.14). At the site scale, the correlation matrix computed between the three detrended chronologies (Fig. S4) showed that the TRW and CD chronologies share between 58 (r=-0.76) and 77% (r=-0.88) of common variability. By contrast, correlations between CD and MLA were only rarely significant. Inter-site correlations computed between TRW chronologies (0.58 - 0.7) were significantly higher than those found between MLA chronologies (0.26 - 0.42).

3.2 Gradient detection

The principal component gradient analyses (PCGA) computed over the 1951-2020 period for the TRW, CD and MLA series showed diverging results (Fig. 3). For TRW, the PCGA differentiates three clusters that are composed primarily of the ring-width series from Bujaleuf, Compreignac and Rochechouart (Fig. 3a). The Wilcoxon rank-sum test confirmed that the non-parametric means of the PCGA loadings of site pairs statistically differ between the three sites. By contrast, it failed to discriminate Saint-Hilaire-les-Places from Bujaleuf and Rochechouart. Results from the leave-one-out analysis showed that 100% of the trees from COM and ROC were assigned to their original sites. By contrast, only 50% of the trees sampled at Bujaleuf were

properly allocated, whereas 40% and 10% were considered to belong to Rochechouart and Compreignac, respectively. The PCGA performed on the spline detrended CD series and the Wilcoxon rank-sum test (Fig. 3b) isolated a cluster composed of trees from Bujaleuf from a second group that indifferently integrated trees from the three other sites. The confusion matrix from the leave-one-out analysis showed that 9 out of 10 trees from Bujaleuf and one tree from HIL were traced back to the above-mentioned cluster. In the case of the MLA series, the PCGA identified a cluster composed of Compreignac series that was distinct from a second group including trees from the three other sites (Fig. 4b). Yet, the leave-one-out analysis, which failed to assign MLA series from Compreignac trees to the correct cluster, confirmed the results.

3.3. Climatic drivers of the PCGA gradients

We then investigated oak climate–growth relationships at the four sites following a two-step procedure. Bootstrap correlation functions were computed in step 1 between the TRW and CD site chronologies over the 1951-2020 period; they showed comparable, albeit inverted, profiles (Fig. S5a, c). At the four sites, TRW and CD are mainly driven by late spring and summer (May (n) – July (n)) and, to a lesser extent, previous August (n-1) and March (n) temperatures. Site comparison shows that RW and CD chronologies from Rochechouart and Saint-Hilaire-les-Places are more sensitive to precipitation than the ones from Bujaleuf and Compreignac. For MLA chronologies, BCFs show more complex and heterogeneous profiles (Fig. S5c) with vessel lumen area being primarily and negatively constrained by spring (march to May (n)) precipitation (Fig. S5b).

In a second step, we explored the climatic drivers of the three (TRW, CD and MLA) gradients retrieved from the PCGAs. In the case of TRW (Fig. 4a), correlation analyses between the gradient derived from the PCGA and climate variables indicate a significant effect of June precipitation and drought index as well as August temperatures on the PCGA gradient. Radial growth in trees from the eastern site (Bujaleuf) are most limited by summer conditions whereas those from the other sites, especially Compreignac, did not show clear dependency. The Wilcoxon rank-sum test shows that the difference between Compreignac and the other sites is statistically significant ($p<0.01$). Similarly, the strength of the climate correlations also varied along the PCGA gradient as derived from CD (Fig. 4b). CD series from the easternmost location (Bujaleuf) show significantly higher correlations with drought (May-Aug) than those from the three other sites. The Wilcoxon rank-sum test

283 also points to significant differences ($p<0.01$) between all site pairs with the exception of
284 Compreignac/Rochechouart. Finally, winter (Feb-Mar) conditions as well as May (n) drought mostly explain the
285 distinction between the MLA series obtained at Compreignac from those obtained at Bujaleuf, Saint-Hilaire-les-
286 Places and Rochechouart (Fig. 4c).

287 ### 3.4 Element concentrations and wood $^{87}Sr/^{86}Sr$ ratios

288 We searched for the presence of a vast suite of major trace and rare earth elements in the twenty trees
289 sampled for geochemical analyses. Due to concentrations below the detection limit, magnesium (Mg), sodium
290 (Na) and silicon (Si) could not be retrieved at the sites. By contrast, concentrations of calcium (Ca) and
291 potassium (K) – representing crucial nutrients of plants – ranged between 0.2 and 2.8 $mg.g^{-1}$. The five trees
292 sampled at Bujaleuf showed fairly low Ca concentrations with values <0.5 $mg.g^{-1}$ whereas this value was
293 exceeded in all trees sampled at Compreignac (Figure 5a). By contrast, no clear inter-site differentiation
294 seemed to exist in terms of K concentrations. Strontium (Sr) and rubidium (Rb) concentrations – both trace
295 elements considered as analogues of Ca and K, respectively – ranged between 1 and 8 $\mu g.g^{-1}$. Concentrations of
296 both elements allowed clear discrimination of all HIL trees – characterized by concentrations in Sr>4.9 and
297 Rb<2.5 $\mu g.g^{-1}$ – from those of the other sites (Compreignac, Bujaleuf and Rochechouart). The other trace
298 elements – i.e. barium (Ba), cadmium (Cd), cobalt (Co), chromium (Cr), copper (Cu), molybdenum (Mo),
299 niobium (Nb), lead (Pb) and lanthanum (La) – were systematically detected in trees but without any significant
300 site signatures. Regarding rare elements, the most striking feature is their absence in trees sampled at
301 Compreignac.

302 Fig. 5b illustrates the ratios of $^{87}Sr/^{86}Sr$, pointing to lower concentrations and the most homogeneous
303 signatures at HIL (0.7096-0.7122, σ=0.001) and ROC (0.7158-0.7177, σ= 0.0008). By contrast, trees from
304 Bujaleuf and Compreignac have higher radiogenic signatures (0.7158-0.7177), but values are also more
305 heterogeneous (σ=0.003 and 0.0013, respectively). The Wilcoxon rank sum test performed between pairs of
306 sites showed that isotopic signatures at Saint-Hilaire-les-Places, Rochechouart and Bujaleuf/Compreignac are
307 statistically different ($p<0.01$), whereas $^{87}Sr/^{86}Sr$ ratios did not differ statistically at Bujaleuf and Compreignac.

4. Discussion

Most studies on dendroprovenancing have hitherto been based on correlation analyses between tree-ring width (TRW) series of trees to be provenanced and networks of reference chronologies. These studies were also often devoted to long-distance timber trade (e.g. Domínguez-Delmás et al., 2014; Fraiture, 2009; Bernabei et al., 2019; Daly et al., 2022), in which case growth patterns between regions may have differed enough to identify distinct growth patterns. In recent years, research on historic timber provenance has increasingly shifted from single-parameter studies to multiproxy approaches (Akhmetzyanov et al., 2019; Akhmetzyanov et al., 2020a; Akhmetzyanov et al. 2020b; Dominguez-Delmas et al., 2020b). In this explorative study, we combined TRW, quantitative wood anatomy and stable strontium isotopes to pinpoint the provenance of wood within central France. The innovative approach has delivered very promising results and has the potential to allow dendroprovenancing at spatial scales that could not so far be addressed with the more conventional approaches.

4.1 The signal retained in tree-ring width series

TRW-climate relations computed at the four stands sampled around the city of Limoges (Haute-Vienne, France) are comparable to those reported by Bose et al. (2021) for oak trees in the Atlantic regions of Europe, especially regarding the positive response of trees to current (n) spring to early summer and, to a lesser extent, to previous (n-1) winter (January) precipitation. This suggests that a macro-climatic signal prevails in this part of Europe (Bose et al., 2021), thereby paving the way for the development of macro-regional chronologies of oak for dating purposes. Yet, such a macro-climatic signal should also limit the potential of TRW chronologies for provenancing purposes (Bridge, 2012). Indeed, the principal component gradient analysis performed on TRW at the four sites only allowed differentiation of the series sampled at the northernmost site (COM) where sensitivity to precipitation as well as drought in spring and early summer seems to be less marked as compared to the three other stands. Yet, the leave-one-out approach in which one tree from BUJ and two trees from HIL sites were erroneously assigned to the COM cluster highlights the limited robustness of TRW-based

discriminations, thereby confirming the shortcoming of TRW series for short-distance, macro-regional dendroprovenancing in the area (Gut, 2018).

4.2 Contribution of wood anatomical features to dendroprovenancing

Oak cell features (e.g. cell diameter or lumen area) have been demonstrated to differ between location or along climate gradients (Fonti and García-Gonzalez, 2004) and to record climatic information where TRW normally fails (for instance at non-marginal sites, where no particular limiting factor prevails, Davies and Loader 2020). Therefore, cell features should – at least theoretically – present a valuable alternative to TRW as they could help to increase the precision of dendroprovenancing studies. Yet, at our sites, the common signal of mean lumen area (MLA) is lower than that of TRW and cell diameter (CD). The Rbar values obtained at HIL and ROC are comparable to those reported for *Quercus robur* L. in Spain (Garcia-Gonzalez and Eckstein, 2003), *Quercus rubra L*. and *Quercus alba L.* in Canada (Tardif et al, 2006), and higher than those obtained for *Castanea sativa* in the southern Swiss Alps (Fonti and Garcia, Gonzalez, 2004; Fonti et al., 2007). Furthermore, the MLA series are less affected by previous growth and consequently less autocorrelated than TRW (as shown in previous studies, for instance Fonti and Garcia-Gonzalez, 2004; Tardif et al., 2006). The MLA series show highly significant negative correlations with precipitation between current (n) March and June and positively correlate with March temperatures. Similar responses of oak trees to spring temperature and precipitation are reported by Fonti and Garcia-Gonzalez (2008) at mesic sites in the Swiss Alps. Despite the agreement with existing studies, PCGA and LOA approaches performed on MLA series successfully isolate trees from COM, more sensitive to winter precipitation (Feb-Mar) and spring (May) drought, but fail to discriminate trees originating from BUJ, HIL and ROC. Contrasted responses of oak vessel series – and thus their potential as a proxy for dendroprovenancing – have hitherto only been documented in regions with strongly contrasting climatic regimes. In Switzerland, Fonti and García-Gonzalez (2004) showed different responses of mean vessel lumen area to climate in oaks growing close to Locarno (1860 mm of annual precipitation), Zurich (1135 mm) and Sion (604 mm). Similarly, in Spain, Akhmetzyanov et al. (2019) used variation in latewood width (LW) and earlywood vessel size to differentiate oak trees growing in the Basque Country (189 mm of precipitation on average) from those living in Cantabrian (650 mm). At our sites, by contrast, the total difference between the

wettest (BUJ, 1078 mm) and the driest (ROC, 914 mm) sites is negligible with only 164 mm, i.e. ~15% of total precipitation. This very small difference in precipitation totals probably explains the lack of similar clear differences in vessel parameters, thereby preventing a clear discrimination of wood anatomical features between sites. Finally, we obtained the most robust and promising results using cell density (CD) series. To our knowledge, this composite index has not been tested so far in dendroprovenancing studies. Computed as the ratio between number of cells and the xylem area, CD series allowed discrimination of three clusters, composed of BUJ, HIL and COM/ROC trees respectively, based on differential correlations with spring/summer drought conditions. Therefore, this parameter has revealed itself as a key tool for the discrimination between sites and we recommend further studies to test it.

4.3 GEOCHEMICAL SIGNATURE AS WOOD PROVENANCE MARKER

Unlike variables dependent of climatic conditions, such as TRW, wood anatomical features and stable oxygen or carbon isotopes, inorganic constituents present in wood are controlled by geological and pedological processes. Through the weathering of rocks, they become available in the soil from where they are taken up by trees (Hajj et al., 2017). In particular, the analysis of strontium (Sr) isotopes in wood offers an interesting, climate-independent alternative to source the origin of wood (Hajj et al, 2017; Dominguez-Delmas et al., 2020b). In Chaco Canyon (New Mexico), for instance, English et al. (2001) and Reynolds et al. (2005) used the $^{87}Sr/^{86}Sr$ ratio to trace the provenance of archeological wood samples from six Puebloan houses. In the Eastern Mediterranean region, Rich et al. (2012) showed distinct Sr signatures in cedar wood (*Cedrus* sp.) from different forests in Lebanon, Cyprus, and Turkey. Yet, this very promising approach to identify wood provenance is not readily applicable everywhere (Bridge, 2012), and it is supposed to be applied to trees that have been sampled at sites with distinct isotopic signatures.

At a given location, $^{87}Sr/^{86}Sr$ signature in trees depends on weathering fluxes from soils and bedrocks and on atmospheric inputs. In this study, all trees were sampled on old plutonic rocks which are supposed to be more radiogenic than atmospheric fluxes (~0.71, Haji et al., 2017) as they contain minerals with high Sr isotopic ratios. Although the rocks have the same origin and are of the same family, our results show that three of the four sites (BUJ-COM, HIL and ROC) are significantly discriminated using the $^{87}Sr/^{86}Sr$ signatures of living trees.

We hypothesize that this discrimination could be explained, on the one hand, by different richness in radiogenic alterable minerals between the different sites, and on the other hand, by a quite homogeneous signature within a given site. This assumption is further supported by field observations (Tab. 2). At COM and BUJ, Sr signatures in trees probably reflect the signatures of soils developed from rocks rich in ferro-magnesian minerals (biotite and/or phlogopite) known to have high Sr isotopic ratios (see Table 1 in Hajj et al. 2017). Conversely, at HIL and ROC, soils and trees developed on soils with low K and radiogenic weatherable minerals.

The limited intra-site variability also explains the discrimination we find in this study. Indeed, the most homogeneous intra-site signature, observed at ROC, probably reflects the relative vicinity of the five sampled trees (on average within 48 meters of each other) and the flat topography which in turn limits geological and edaphic variations. By contrast, the highest (albeit also small) variability observed at BUJ probably results from the larger spread of sampled trees (120 m on average between the sampled trees). At this site, the two trees (BUJ 12 and BUJ 14) with higher $^{87}Sr/^{86}Sr$ ratios were indeed sampled on a hilltop characterized by different lithology. At COM, trees were sampled at a site characterized by thick soils as well as comparable elevation and slope aspect. We hypothesize that the small intra-site variability observed in this case may result from a Sr isotopic gradient across the soil, with lower ratios resulting from atmospheric deposition at the soil surface and higher signatures explained by increasing weathering contribution closer to the bedrock. In such a setting, trees with deeper root systems will uptake water and nutrients with higher Sr isotopic ratios, and may thus have different isotopic signatures (Dambrine et al., 1997; Poszwa et al. 2002). Yet, we do not have any information on the root system of the sampled trees, and therefore checked for potential relationships between Sr isotopic ratios, tree age (Fig. S6a) and diameter (Fig. S6b), and annual radial increment, with the latter being considered to indirectly reflect the dominance status of a tree (Fig. S6c). However, this analysis did not yield any clear trend that would support our assumption.

Finally, as $^{87}Sr/^{86}Sr$ ratios failed to discriminate trees from BUJ and COM, we tested Ca and K concentrations as potential geochemical tracers. Our results show that Ca concentrations differ significantly between BUJ and COM (Fig. 5a). When combined with Sr ratios (Fig. 5b), we argue that a multi-proxy approach combining Sr and Ca concentration ratios in historical woods represents a very valuable, additional tracer to increase the

precision of dendroprovenancing. In that respect, we encourage future studies to couple isotopic and major trace elements analyses more systematically.

5 CONCLUSION

Over the last decade, the increasing need to identify the origin of wood from temperate and tropical forests with high geographical resolution has propelled the development of novel proxies for wood provenancing and implementation of combined scientific approaches. Here, we coupled tree-ring width measurements, quantitative wood anatomy and geochemical signatures to increase the precision of dendroprovenancing at the local scale, as this would inform science on the utilization of domestic forests as well as on historical management practices over the past millennium and beyond. We demonstrate that the coupling of cell density – a wood anatomical index introduced to dendroprovenancing in this study – with geochemical signatures (i.e. the $^{87}Sr/^{86}Sr$ isotopic and Sr/Ca element ratios) allows pinpointing to the origin of oak timbers originating from four stands sampled around the city of Limoges. This is a remarkable outcome in view of the small geographic scale of the research area, with very limited differences in elevation, temperature and rainfall between sites, and where complacent tree growth is only interrupted by signals that can be attributed to forest management (e.g., coppicing). The findings of this study are therefore considered to have great implications on studies focusing on historical timbers from domestic forests, as any determination of their origin with high geographical resolution will represent a crucial step forward in our understanding of the success or failure of forest management practices in past centuries; the lessons learnt can in turn serve to inform current policies in European forests. This study therefore also calls for replication in other regions and the inclusion of other species and tree-ring variables so as to ensure repeatability and reproducibility of the approach developed here. Although diffuse porous species are characterized by an early to latewood transition more difficult to identify, we believe that the approach used in this study could be adopted for such species as well. As regards conifers, maximum latewood density (MXD) and maximum latewood radial cell wall thickness (CWTrad) would be good variables to use for dendroprovenancing studies, as it was demonstrated that they are reliable proxies for past climate variability reconstruction (Björklund et al., 2020; Lopez-Saez et al., 2023). Nevertheless, it has

to be noted that the smaller size of cells in both diffuse porous and conifer species would require the preparation of thin sections, which would increase the time needed to complete the wood anatomical analysis.

Acknowledgements

We thank Danièle Bartier for helping during fieldwork and for providing a detailed description and interpretation of the geological context; our colleagues Elise Guérin, Camille Kieffer, Delphine Yeghicheyan, Catherine Zimmermann and Christophe Cloquet (SARM Nancy) for the geochemical analyses; the C-CIA group of the University of Geneva for giving unvaluable advice on how to use the ROXAS and the R studio software; Allan Buras for providing the code of the principal component gradient analysis (PCGA), as well as an online video tutorial on how to use it (https://dendroschool.org/multivariate-statistics-in-tree-ring-analyses-coming-soon/). Finally, we would like to thank the Association for Tree-Ring Research (ATR) for organizing the 31st European Dendroecological Fieldweek (Val Müstair, September 2021), which represented a precious opportunity for scientific discussion, and for providing the travel fundings which made it possible to present these results at the congress "From Forests to Heritage" (Amsterdam, 19-21 April 2022).

Fundings

This work has been supported by the Service *Régional de l'Archéologie* (SRA) of the Region Nouvelle-Aquitaine (France).

Bibliography

- Akhmetzyanov, L., Buras, A., Sass-Klaassen, U., den Ouden, J., Mohren, F., Groenendijk, P., & García-González, I. (2019). Multi-variable approach pinpoints origin of oak wood with higher precision. *Journal of Biogeography*, *46*(6), 1163–1177. https://doi.org/10.1111/jbi.13576.
- Akhmetzyanov, L., Copini, P., Sass-Klaassen, U., Schroeder, H., de Groot, G. A., Laros, I., & Daly, A. (2020a). DNA of centuries-old timber can reveal its origin. *Scientific Reports*, *10*(1), 1–10. https://doi.org/10.1038/s41598-020-77387-2.

- Akhmetzyanov, L., Sánchez-Salguero, R., García-González, I., Buras, A., Dominguez-Delmás, M., Mohren, F., den Ouden, J., & Sass-Klaassen, U. (2020b). Towards a new approach for dendroprovenancing pines in the Mediterranean Iberian Peninsula. *Dendrochronologia*, *60*(January), 125688. https://doi.org/10.1016/j.dendro.2020.125688.
- Alla, A. Q., & Camarero, J. J. (2012). Contrasting responses of radial growth and wood anatomy to climate in a Mediterranean ring-porous oak: Implications for its future persistence or why the variance matters more than the mean. *European Journal of Forest Research*, *131*(5), 1537–1550. https://doi.org/10.1007/s10342-012-0621-x.
- Baillie M. G. L. (1982). Tree-Ring Dating and Archaeology. University of Chicago Press, Chicago.
- Bernabei, M., Bontadi, J., Rea, R., Büntgen, U., & Tegel, W. (2019). Dendrochronological evidence for long-distance timber trading in the Roman Empire. *PLoS ONE*, *14*(12). https://doi.org/10.1371/journal.pone.0224077.
- Björklund, J., Seftigen, K., Fonti, P., Nievergelt, D., & von Arx, G. (2020). Dendroclimatic potential of dendroanatomy in temperature-sensitive Pinus sylvestris. *Dendrochronologia*, *60*(February), 125673. https://doi.org/10.1016/j.dendro.2020.125673.
- Bose, A. K., Scherrer, D., Camarero, J. J., Ziche, D., Babst, F., Bigler, C., Bolte, A., Dorado-Liñán, I., Etzold, S., Fonti, P., Forrester, D. I., Gavinet, J., Gazol, A., de Andrés, E. G., Karger, D. N., Lebourgeois, F., Lévesque, M., Martínez-Sancho, E., Menzel, A., Rigling, A. (2021). Climate sensitivity and drought seasonality determine post-drought growth recovery of Quercus petraea and Quercus robur in Europe. *Science of the Total Environment*, *784*, 147222. https://doi.org/10.1016/j.scitotenv.2021.147222.
- Bräker, O. U. (2002). Measuring and data processing in tree-ring research – a methodological introduction, *Dendrochronologia, 20*(2002), pp. 203–216. https://doi.org/10.1078/1125-7865-00017.
- Bridge, M. (2012). Locating the origins of wood resources: A review of dendroprovenancing. *Journal of Archaeological Science*, *39*(8), 2828–2834. https://doi.org/10.1016/j.jas.2012.04.028.
- Büntgen, U., Tegel, W., Nicolussi, K., McCormick, M., Frank, D., Trouet, V., Kaplan, J. O., Herzig, F., Heussner, K. U., Wanner, H., Luterbacher, J., & Esper, J. (2011). 2500 years of European climate variability and human susceptibility. *Science*, *331*(6017), 578–582. https://doi.org/10.1126/science.1197175.

- Buras, A. (2017). A comment on the expressed population signal. *Dendrochronologia*, *44*, 130–132. https://doi.org/10.1016/j.dendro.2017.03.005.
- Buras, A., Van Der Maaten-Theunissen, M., Van Der Maaten, E., Ahlgrimm, S., Hermann, P., Simard, S., Heinrich, I., Helle, G., Unterseher, M., Schnittler, M., Eusemann, P., & Wilmking, M. (2016). Tuning the voices of a choir: Detecting ecological gradients in time-series populations. *PLoS ONE*, *11*(7), 1–21. https://doi.org/10.1371/journal.pone.0158346.
- Bunn, A. G. (2008). A dendrochronology program library in R (dplR). *Dendrochronologia*, *26*(2), 115–124. https://doi.org/10.1016/j.dendro.2008.01.002.
- Campelo, F., Nabais, C., Gutiérrez, E., Freitas, H., García González, I. (2010). Vessel features of *Quercus Ilex* L. growing under Mediterranean climate have a better climatic signal than tree-ring width. *Trees* 24: 463-470. https://doi.org/10.1007/s00468-010-0414-0.
- Castagneri, D., Petit, G., & Carrer, M. (2015). Divergent climate response on hydraulic-related xylem anatomical traits of Picea abies along a 900-m altitudinal gradient. *Tree Physiology*, *35*(12), 1378–1387. https://doi.org/10.1093/treephys/tpv085
- Crivellaro, A., & Ruffinatto, F. (2020). Wood identification to combat illegal timber trade: the situation in Italy. *Forest@ - Rivista Di Selvicoltura Ed Ecologia Forestale*, *17*(1), 88–91. https://doi.org/10.3832/efor3678-017.
- Crivellaro, A., Schweingruber, F. H., Christodoulou, C.S., Papachristophorou, T., Tsintides, T., Da Ros, A. (2013). Atlas of Wood, Bark and Pith Anatomy of Eastern Mediterranean Trees and Shrubs: with a special focus on Cyprus.
- Corcuera, L., Camarero, J. J., & Gil-Pelegrín, E. (2004). Effects of a severe drought on growth and wood anatomical properties of Quercus faginea. *IAWA Journal*, *25*(2), 185–204. https://doi.org/10.1163/22941932-90000360.
- Cornes, R. C., van der Schrier, G., van den Besselaar, E. J. M., & Jones, P. D. (2018). An Ensemble Version of the E-OBS Temperature and Precipitation Data Sets. *Journal of Geophysical Research: Atmospheres*, *123*(17), 9391–9409. https://doi.org/10.1029/2017JD028200

- Daly, A., Domínguez-Delmás, M., & van Duivenvoorde, W. (2021). Batavia shipwreck timbers reveal a key to Dutch success in 17th-century world trade. *PLoS ONE*, *16*(10 October), 1–17. https://doi.org/10.1371/journal.pone.0259391.
- Daly, A., & Tyers, I. (2022). The sources of Baltic oak. *Journal of Archaeological Science*, *139*(January), 105550. https://doi.org/10.1016/j.jas.2022.105550.
- Dambrine, E., Loubet, M., Vega, J. A., & Lissarague, A. (1997). Localisation of mineral uptake by roots using Sr isotopes. *Plant and Soil*, *192*(1), 129–132. https://doi.org/10.1023/A:1004294820733.
- Davies, D., & Loader, N. J. (2020). An evaluation of english oak earlywood vessel area as a climate proxy in the UK. *Dendrochronologia*, *64*(October), 125777. https://doi.org/10.1016/j.dendro.2020.125777.
- Domínguez-Delmás, M. (2020a). Seeing the forest for the trees: New approaches and challenges for dendroarchaeology in the 21st century. *Dendrochronologia*, *62*(October 2019), 125731. https://doi.org/10.1016/j.dendro.2020.125731.
- Domínguez-Delmás, M., Rich, S., Traoré, M., Hajj, F., Poszwa, A., Akhmetzyanov, L., García-González, I., & Groenendijk, P. (2020b). Tree-ring chronologies, stable strontium isotopes and biochemical compounds: Towards reference datasets to provenance Iberian shipwreck timbers. *Journal of Archaeological Science: Reports*, *34*. https://doi.org/10.1016/j.jasrep.2020.102640.
- Domínguez-Delmás, M., Driessen, M., García-González, I., van Helmond, N., Visser, R., & Jansma, E. (2014). Long-distance oak supply in mid-2nd century AD revealed: The case of a Roman harbour (Voorburg-Arentsburg) in the Netherlands. *Journal of Archaeological Science*, *41*, 642–654. https://doi.org/10.1016/j.jas.2013.09.009.
- Dormontt, E. E., Boner, M., Braun, B., Breulmann, G., Degen, B., Espinoza, E., Gardner, S., Guillery, P., Hermanson, J. C., Koch, G., Lee, S. L., Kanashiro, M., Rimbawanto, A., Thomas, D., Wiedenhoeft, A. C., Yin, Y., Zahnen, J., & Lowe, A. J. (2015). Forensic timber identification: It's time to integrate disciplines to combat illegal logging. *Biological Conservation*, *191*, 790–798. https://doi.org/10.1016/j.biocon.2015.06.038.
- Drake, B. L. (2018). Source & Sourceability: Towards a probabilistic framework for dendroprovenance based on hypothesis testing and Bayesian inference. *Dendrochronologia*, *47*(March 2017), 38–47. https://doi.org/10.1016/j.dendro.2017.12.004.

- Eckstein, D., & Wrobel, S. (2007). Dendrochronological proof of origin of historic timber–retrospect and perspectives. *TRACE - Proceedings of the Symposium on Tree Rings in Archaeology, Climatology and Ecology*, *5* (2007), pp. 8–20.
- Eilmann, B., Zweifel, R., Buchmann, N., Graf Pannatier, E., & Rigling, A. (2011). Drought alters timing, quantity, and quality of wood formation in Scots pine. *Journal of Experimental Botany*, *62*(8), 2763–2771. https://doi.org/10.1093/jxb/erq443.
- English, N. B., Betancourt, J. L., Dean, J. S., & Quade, J. (2001). Strontium isotopes reveal distant sources of architectural timber in Chaco Canyon, New Mexico. *Proceedings of the National Academy of Sciences of the United States of America*, *98*(21), 11891–11896. https://doi.org/10.1073/pnas.211305498.
- Fritts, H. C. (1976). Tree Rings and Climate. Academic Press, London.
- Fowler, A. M., & Bridge, M. C. (2015). Mining the British Isles oak tree-ring data set. Part A: Rationale, data, software, and proof of concept. *Dendrochronologia*, *35*, 24–33. https://doi.org/10.1016/j.dendro.2015.05.008.
- Fraiture, P. (2009). Contribution of dendrochronology to understanding of wood procurement sources for panel paintings in the former Southern Netherlands from 1450 AD to 1650 AD. *Dendrochronologia*, *27*(2), 95–111. https://doi.org/10.1016/j.dendro.2009.06.002.
- Fonti, P., & García-González, I. (2008). Earlywood vessel size of oak as a potential proxy for spring precipitation in mesic sites. *Journal of Biogeography*, *35*(12), 2249–2257. https://doi.org/10.1111/j.1365-2699.2008.01961.x.
- Gasson, P., Baas, P. & Wheeler, E. (2011). Wood anatomy of cities-listed tree species. *IAWA J., 32*(2), pp. 155–198. https://doi.org/10.1163/22941932-90000050.
- García González, I., & Eckstein, D. (2003). Climatic signal of earlywood vessels of oak on a maritime site. *Tree Physiology*, *23*(7), 497–504. https://doi.org/10.1093/treephys/23.7.497.
- García-González, I., Souto-Herrero, M., & Campelo, F. (2016). Ring-porosity and earlywood vessels: a review on extracting environmental information through time. *IAWA Journal*, *37*(2), 295–314. https://doi.org/10.1163/22941932-20160135.

- Gori, Y., Wehrens, R., La Porta, N., & Camin, F. (2015). Oxygen and hydrogen stable isotope ratios of bulk needles reveal the geographic origin of Norway spruce in the European Alps. *PLoS ONE*, *10*(3). https://doi.org/10.1371/journal.pone.0118941.
- Gut, U. (2018). Evaluating the key assumptions underlying dendro-provenancing: How to spruce it up with a scissor plot. *Dendrochronologia*, *52*(April), 131–145. https://doi.org/10.1016/j.dendro.2018.09.008.
- Gut, U. (2020). Assessing site signal preservation in reference chronologies for dendro-provenancing. *PLoS ONE*, *15*(9 September), 1–25. https://doi.org/10.1371/journal.pone.0239425.
- Hajj, F., Poszwa, A., Bouchez, J., & Guérold, F. (2017). Radiogenic and "stable" strontium isotopes in provenance studies: A review and first results on archaeological wood from shipwrecks. *Journal of Archaeological Science*, *86*, 24–49. https://doi.org/10.1016/j.jas.2017.09.005.
- Hao, Y., Wang, Q., Zhang, S. (2021). Rapid Identification of Wood Species Based on Portable Near-Infrared Spectrometry and Chemometrics Methods. *Spettroscopy Supplements, Advances in UV-vis-NIR Spectroscopy, 36*(2021), pp. 7-13.
- Haneca, K., Čufar, K., & Beeckman, H. (2009). Oaks, tree-rings and wooden cultural heritage: a review of the main characteristics and applications of oak dendrochronology in Europe. *Journal of Archaeological Science*, *36*(1), 1–11. https://doi.org/10.1016/j.jas.2008.07.005.
- Haneca, K., Wazny, T., Van Acker, J., & Beeckman, H. (2005). Provenancing Baltic timber from art historical objects: Success and limitations. *Journal of Archaeological Science*, *32*(2), 261–271. https://doi.org/10.1016/j.jas.2004.09.005.
- Kagawa, A., & Leavitt, S. W. (2010). Stable carbon isotopes of tree rings as a tool to pinpoint the geographic origin of timber. *Journal of Wood Science*, *56*(3), 175–183. https://doi.org/10.1007/s10086-009-1085-6.
- Kames, S., Tardif, J. C., & Bergeron, Y. (2011). Anomalous earlywood vessel lumen area in black ash (Fraxinus nigra Marsh.) tree rings as a potential indicator of forest fires. *Dendrochronologia*, *29*(2), 109–114. https://doi.org/10.1016/j.dendro.2009.10.004.
- Kelly, P.M., Munro, M.A.R., Hughes, M.K., Goodess, C.M. (1989). Climate and signature years in west European oaks. *Nature, 340*(1989), pp. 57–60.

- Kniesel, B. M., Günther, B., Roloff, A., & von Arx, G. (2015). Defining ecologically relevant vessel parameters in Quercus robur L. for use in dendroecology: a pointer year and recovery time case study in Central Germany. *Trees - Structure and Function*, *29*(4), 1041–1051. https://doi.org/10.1007/s00468-015-1183-6.
- Kolb, K. J., & Sperry, J. S. (1999). Transport constraints on water use by the Great Basin shrub, Artemisia tridentata. *Plant, Cell and Environment*, *22*(8), 925–935. https://doi.org/10.1046/j.1365-3040.1999.00458.x.
- Jevšenak, J., Džeroski, S., & Levanic, T. (2018). Predicting the vessel lumen area tree-ring parameter of *Quercus robur* with linear and nonlinear machine learning algorithms. *Geochronometria*, *45*(1), 211–222. https://doi.org/10.1515/geochr-2015-0097.
- Leavitt, S. W. (1993). Environmental information from 13C/12C ratios of wood. *Geophysical Monograph*, *78*, 325–331. https://doi.org/10.1029/GM078p0325.
- Levanič, T. (2007). ATRICS - A new system for image acquisition in dendrochronology. *Tree-Ring Research*, *63*(2), 117–122. https://doi.org/10.3959/1536-1098-63.2.117.
- Lopez-Saez, J., Corona, C., von Arx, G., Fonti, P., Slamova, L., & Stoffel, M. (2023). Tree-ring anatomy of Pinus cembra trees opens new avenues for climate reconstructions in the European Alps. *Science of the Total Environment*, *855*(September 2022), 158605. https://doi.org/10.1016/j.scitotenv.2022.158605.
- Lowe, A. J., & Cross, H. B. (2011). The application of DNA methods to timber tracking and origin verification. *IAWA Journal*, *32*(2), 251–262. https://doi.org/10.1163/22941932-90000055.
- Lugli, F., Cipriani, A., Bruno, L., Ronchetti, F., Cavazzuti, C., & Benazzi, S. (2022). A strontium isoscape of Italy for provenance studies. *Chemical Geology*, *587*(October 2021), 120624. https://doi.org/10.1016/j.chemgeo.2021.120624.
- Matisons, R., Elferts, D., & Brumelis, G. (2012). Changes in climatic signals of English oak tree-ring width and cross-section area of earlywood vessels in Latvia during the period 1900-2009. *Forest Ecology and Management*, *279*, 34–44. https://doi.org/10.1016/j.foreco.2012.05.029.
- McCarroll, D., & Loader, N. J. (2004). Stable isotopes in tree rings. *Quaternary Science Reviews*, *23*(7–8), 771–801. https://doi.org/10.1016/j.quascirev.2003.06.017.

- Meko, M. D., & Therrell, M. D. (2020). A record of flooding on the White River, Arkansas derived from tree-ring anatomical variability and vessel width. *Physical Geography*, *41*(1), 83–98. https://doi.org/10.1080/02723646.2019.1677411.
- Mickaël, H., Michaël, A., Fabrice, B., Pierre, M., & Thibaud, D. (2007). Soil detritivore macro-invertebrate assemblages throughout a managed beech rotation. *Annals of Forest Science*, *64*, 219–228. https://doi.org/10.1051/forest.
- Paredes-Villanueva, K., de Groot, G. A., Laros, I., Bovenschen, J., Bongers, F., & Zuidema, P. A. (2019). Genetic differences among Cedrela odorata sites in Bolivia provide limited potential for fine-scale timber tracing. *Tree Genetics and Genomes*, *15*(3). https://doi.org/10.1007/s11295-019-1339-4.
- Poszwa, A., Dambrine, E., Ferry, B., Pollier, B., & Loubet, M. (2002). Do deep tree roots provide nutrients to the tropical rainforest? *Biogeochemistry*, *60*(1), 97–118. https://doi.org/10.1023/A:1016548113624.
- Pritzkow, C., Wazny, T., Heußner, K. U., Słowiński, M., Bieber, A., Liñán, I. D., Helle, G., & Heinrich, I. (2016). Minimum winter temperature reconstruction from average earlywood vessel area of European oak (Quercus robur) in N-Poland. *Palaeogeography, Palaeoclimatology, Palaeoecology*, *449*, 520–530. https://doi.org/10.1016/j.palaeo.2016.02.046.
- Puchałka, R., Koprowski, M., Przybylak, J., Przybylak, R., & Dąbrowski, H. P. (2016). Did the late spring frost in 2007 and 2011 affect tree-ring width and earlywood vessel size in Pedunculate oak (Quercus robur) in northern Poland? *International Journal of Biometeorology*, *60*(8), 1143–1150. https://doi.org/10.1007/s00484-015-1107-6.
- R Core Team (2016). R: A Language and Environment for Statistical Computing. R Foundation for Statistical Computing. R Foundation for Statistical Computing: Vienna. http://www.R-project.org/.
- R Core Team (2020). R: A Language and Environment for Statistical Computing. R Foundation for Statistical Computing. R Foundation for Statistical Computing: Vienna. http://www.R-project.org/.
- Reynolds, A. C., Betancourt, J. L., Quade, J., Patchett, P. J., Dean, J. S., & Stein, J. (2005). 87Sr/86Sr sourcing of ponderosa pine used in Anasazi great house construction at Chaco Canyon, New Mexico. *Journal of Archaeological Science*, *32*(7), 1061–1075. https://doi.org/10.1016/j.jas.2005.01.016.

- Rich, S., Manning, S. W., Degryse, P., Vanhaecke, F., Latruwe, K., & Van Lerberghe, K. (2016a). To put a cedar ship in a bottle: Dendroprovenancing three ancient East Mediterranean watercraft with the 87Sr/86Sr isotope ratio. *Journal of Archaeological Science: Reports*, *9*, 514–521. https://doi.org/10.1016/j.jasrep.2016.08.034.
- Rich, S., Manning, S. W., Degryse, P., Vanhaecke, F., & Van Lerberghe, K. (2016b). Provenancing East Mediterranean cedar wood with the $^{87}Sr/^{86}Sr$ strontium isotope ratio. *Archaeological and Anthropological Sciences*, *8*(3), 467–476. https://doi.org/10.1007/s12520-015-0242-7.
- Ruffinatto, F., & Crivellaro, A. (2019). Atlas of Macroscopic Wood Identification. In *Atlas of Macroscopic Wood Identification*. https://doi.org/10.1007/978-3-030-23566-6.
- Scoch, W., Heller, I., Schweingruber, F. H., Kienast, F. (2004). Wood anatomy of Central European Species. Online version. www.woodanatomy.ch.
- Schroeder, H., Cronn, R., Yanbaev, Y., Jennings, T., Mader, M., Degen, B., & Kersten, B. (2016). Development of molecular markers for determining continental origin of wood from White Oaks (Quercus L. sect. Quercus). *PLoS ONE*, *11*(6), 1–15. https://doi.org/10.1371/journal.pone.0158221.
- Schweingruber, F. H. (1996). Tree Rings and Environment. Dendroecology. Paul Haupt Verlag, Berne.
- Souto-Herrero, M., Rozas, V., & García-González, I. (2017). A 481-year chronology of oak earlywood vessels as an age-independent climatic proxy in NW Iberia. *Global and Planetary Change*, *155*(May), 20–28. https://doi.org/10.1016/j.gloplacha.2017.06.003.
- Speirs, A. K., McConnachie, G., & Lowe, A. J. (2009). Chloroplast DNA from 16th century waterlogged oak in a marine environment: initial steps in sourcing the Mary Rose timbers. *Archaeological Science Under a Microscope: Studies in Residue and Ancient DNA Analysis in Honour of Thomas H. Loy*, 175–189. https://doi.org/10.22459/ta30.07.2009.13.
- Tardif, J. C., Conciatori, F., Nantel, P., & Gagnon, D. (2006). Radial growth and climate responses of white oak (Quercus alba) and northern red oak (Quercus rubra) at the northern distribution limit of white oak in Quebec, Canada. *Journal of Biogeography*, *33*(9), 1657–1669. https://doi.org/10.1111/j.1365-2699.2006.01541.x.

- Tegel, W., Muigg, B., Skiadaresis, G., Vanmoerkerke, J., & Seim, A. (2022). Dendroarchaeology in Europe. *Frontiers in Ecology and Evolution*, *10*(February). https://doi.org/10.3389/fevo.2022.823622.
- Traoré, M., Kaal, J., & Martínez Cortizas, A. (2018). Chemometric tools for identification of wood from different oak species and their potential for provenancing of Iberian shipwrecks (16th-18th centuries AD). *Journal of Archaeological Science*, *100*(January), 62–73. https://doi.org/10.1016/j.jas.2018.09.008.
- Tyree, M. T., & Ewers, F. W. (1991). The hydraulic architecture of trees and other woody plants. *New Phytol*. 119, 345–360.
- Van Ham-Meert, A., Rodler, A. S., Waight, T. E., & Daly, A. (2020). Determining the Sr isotopic composition of waterlogged wood – Cleaning more is not always better. *Journal of Archaeological Science*, *124*, 105261. https://doi.org/10.1016/j.jas.2020.105261.
- Vicente-Serrano, S. M., Beguería, S., Lorenzo-Lacruz, J., Camarero, J. J., López-Moreno, J. I., Azorin-Molina, C., Revuelto, J., Morán-Tejeda, E., & Sanchez-Lorenzo, A. (2012). Performance of drought indices for ecological, agricultural, and hydrological applications. *Earth Interactions*, *16*(10), 1–27. https://doi.org/10.1175/2012EI000434.1.
- von Arx, G., & Carrer, M. (2014). Roxas -A new tool to build centuries-long tracheid-lumen chronologies in conifers. *Dendrochronologia*, *32*(3), 290–293. https://doi.org/10.1016/j.dendro.2013.12.001.
- Von Arx, G., Crivellaro, A., Prendin, A. L., Čufar, K., & Carrer, M. (2016). Quantitative wood anatomy — practical guidelines. *Frontiers in Plant Science*, *7*(June 2016), 1–13. https://doi.org/10.3389/fpls.2016.00781.
- Wazny, T. (2002). Baltic timber in Western Europe - An exciting dendrochronological question. *Dendrochronologia*, *20*(3), 313–320. https://doi.org/10.1078/1125-7865-00024.
- Wigley, T. M. L., Briffa, K. R. & Jones, P. D. (1984). On the average value of correlated time series, with applications in dendroclimatology and hydrometeorology. *Journal of Applied Meteorology and Climatology, 23*(2), 201-213. https://doi.org/10.1175/1520-0450(1984)023<0201:OTAVOC>2.0.CO;2.
- Zang, C., & Biondi, F. (2015). Treeclim: An R package for the numerical calibration of proxy-climate relationships. *Ecography*, *38*(4), 431–436. https://doi.org/10.1111/ecog.01335.
- Ziaco, E., Liang, E. (2019). New perspectives on sub-seasonal xylem anatomical responses to climatic variability. *Trees* 33, 973–975 (2019). https://doi.org/10.1007/s00468-018-1786-9.

694 • Ziaco, E., Biondi, F., Heinrich, I. (2016). Wood Cellular Dendroclimatology: Testing New Proxies in Great Basin
695 Bristlecone Pine. *Frontiers in Plant Science*, 1(7). https://doi.org/10.3389/fpls.2016.01602.
696 • Zweifel R., Zeugin F., Zimmermann L. & Newbery D.M. (2006). Intra-annual radial growth and water relations
697 of trees – implications towards a growth mechanism. *Journal of Experimental Botany* 57(2006), pp. 1445–
698 1459.
699

700 ## FIGURES

701 **Fig. 1.** The four study sites are located in the Nouvelle Aquitaine Region in a radius of 30 km around the city of
702 Limoges (a). At each site, 20 to 30 dominant oak trees were sampled. Panel b shows the distribution of ● trees
703 which have been sampled for tree-ring analyses; ● for tree-ring width and isotope analyses; ◆ for tree-ring
704 width and wood anatomical analyses; ◆ for tree-ring width, wood anatomical and isotopic analyses. Panel c
705 shows climate diagram of each site according to the 0.1 x 0.1 lat/long E-OBS gridded data set.

706 **Fig.2.** Ring- width spline detrended chronologies (lower panel) and Express Population Signal (EPS, upper panel)
707 computed across a 30-year moving window with a 29-year overlap for the Bujaleuf (a), Compreignac (b), Saint-
708 Hilaire-les-Places (c) and Rochechouart (d) sites.

709 **Fig. 3.** Principal Component Gradient analysis (upper panel), Wilcoxon rank-sum test matrixes (central panel)
710 and leave-one-out approaches computed for ring width (RW, left panel), cell density (CD, central panel) and
711 mean lumen area (MLA, right) series of Bujaleuf (BUJ), Compreignac (COM), Rochechouart (ROC) and Saint-
712 Hilaire-les-Places (HIL) sites.

713 **Fig. 4.** Relationships between monthly climate variables and the principal component gradient analyses (PCGA)-
714 rank (upper panel) derived from ring width (RW), cell density (CD) and mean lumen area (MLA) time series of
715 Bujaleuf (BUJ), Compreignac (COM), Rochechouart (ROC) and Saint-Hilaire-les-Places (HIL). Correlations
716 between individual TRW, CD and MLA series and August temperature (left lower panel), May-August SPEI
717 (central lower panel) and May SPEI (right lower panel). Boxplots in the lower panel show the distributions of
718 correlations of individual series with August temperature, May-August and May SPEI.

719 **Fig.5.** Geochemical and isotope analyses. Calcium concentrations (a) and strontium isotopic ratios (b) in the
720 wood from trees sampled at Bujaleuf (BUJ), Compreignac (COM), Saint-Hilaire-les-Places (HIL) and
721 Rochechouart (ROC) sites.

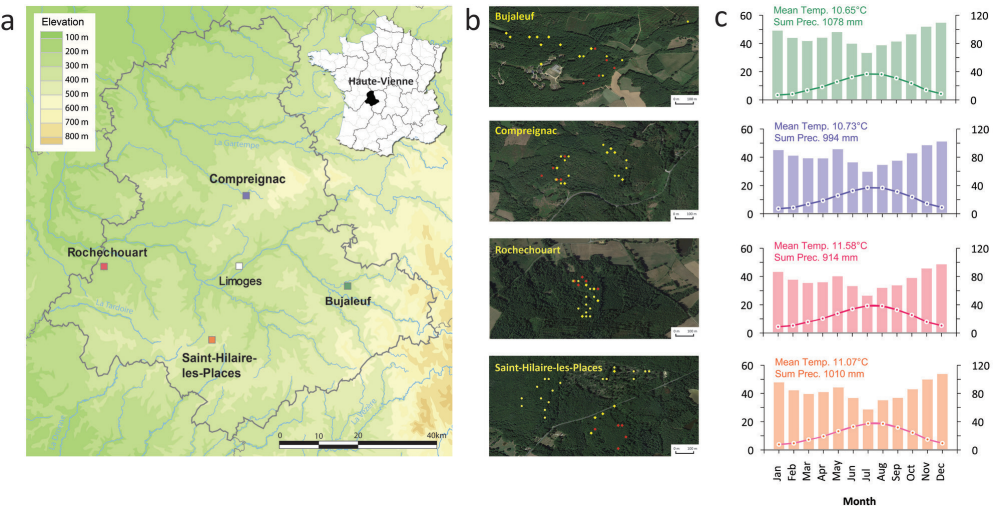
a
Elevation
100 m
200 m
300 m
400 m
500 m
600 m
700 m
800 m
Haute-Vienne
Compreignac
Rochechouart
Limoges
Bujaleuf
Saint-Hilaire-
les-Places
0
10
20
40km
b
Bujaleuf
Compreignac
Rochechouart
Saint-Hilaire-les-Places
c
Mean Temp. 10.65°C
Sum Prec. 1078 mm
Mean Temp. 10.73°C
Sum Prec. 994 mm
Mean Temp. 11.58°C
Sum Prec. 914 mm
Mean Temp. 11.07°C
Sum Prec. 1010 mm
Jan
Feb
Mar
Apr
May
Jun
Jul
Aug
Sep
Oct
Nov
Dec
Month

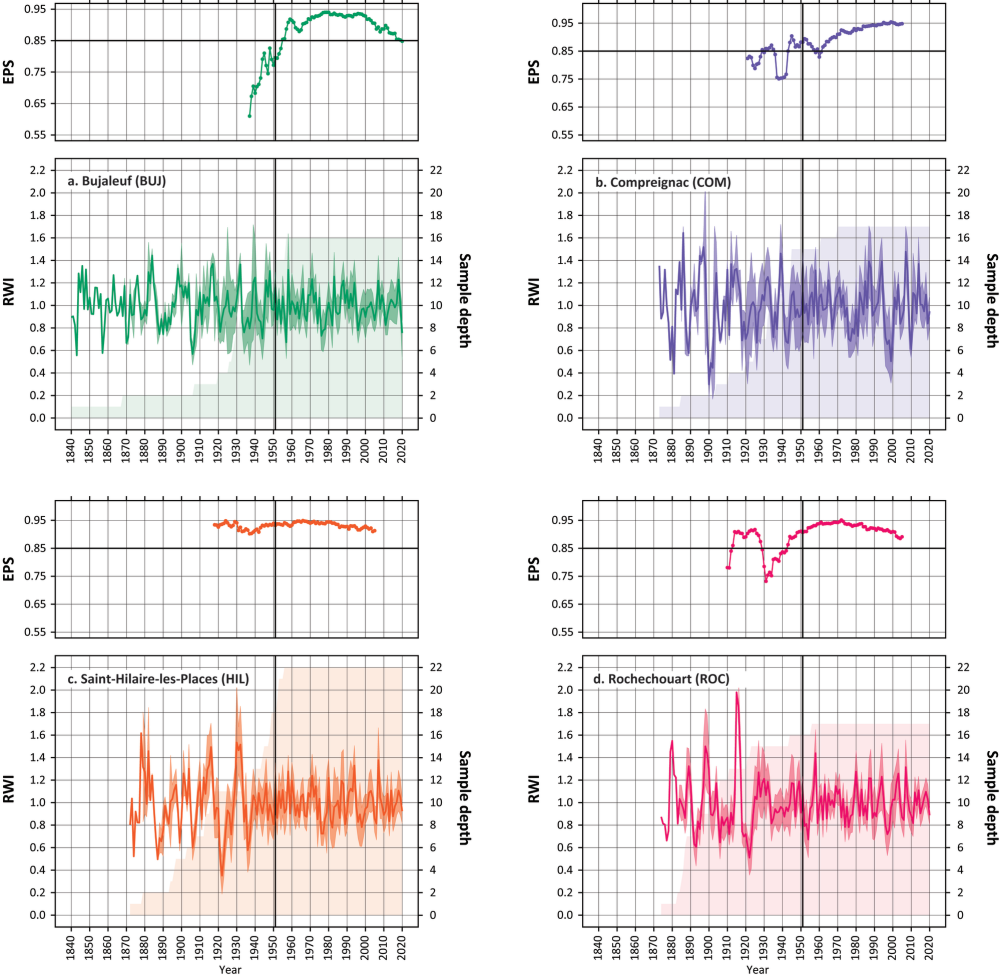
EPS
RWI
Sample depth
a. Bujaleuf (BUJ)
b. Compreignac (COM)
c. Saint-Hilaire-les-Places (HIL)
d. Rochechouart (ROC)
Year

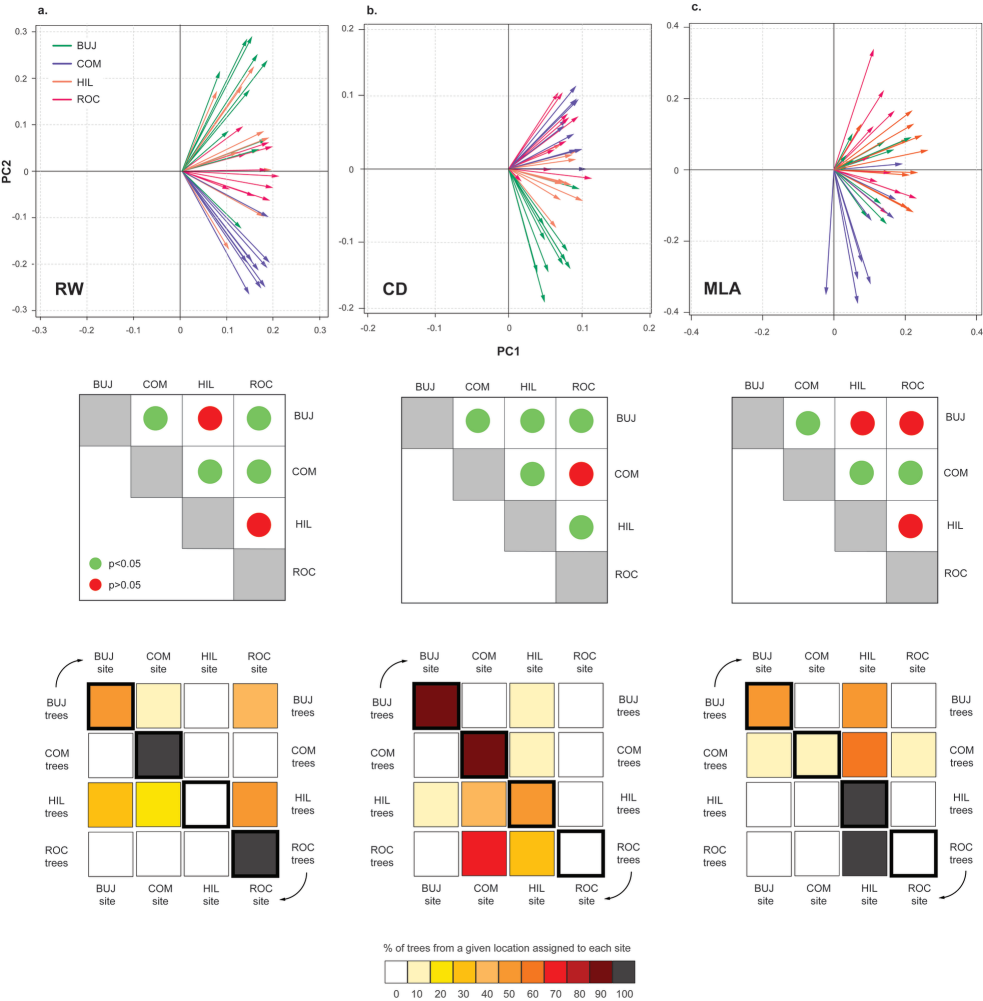
a.
b.
c.
BUJ
COM
HIL
ROC
RW
CD
MLA
PC1
PC2
p<0.05
p>0.05
BUJ site
COM site
HIL site
ROC site
BUJ trees
COM trees
HIL trees
ROC trees
% of trees from a given location assigned to each site
0 10 20 30 40 50 60 70 80 90 100

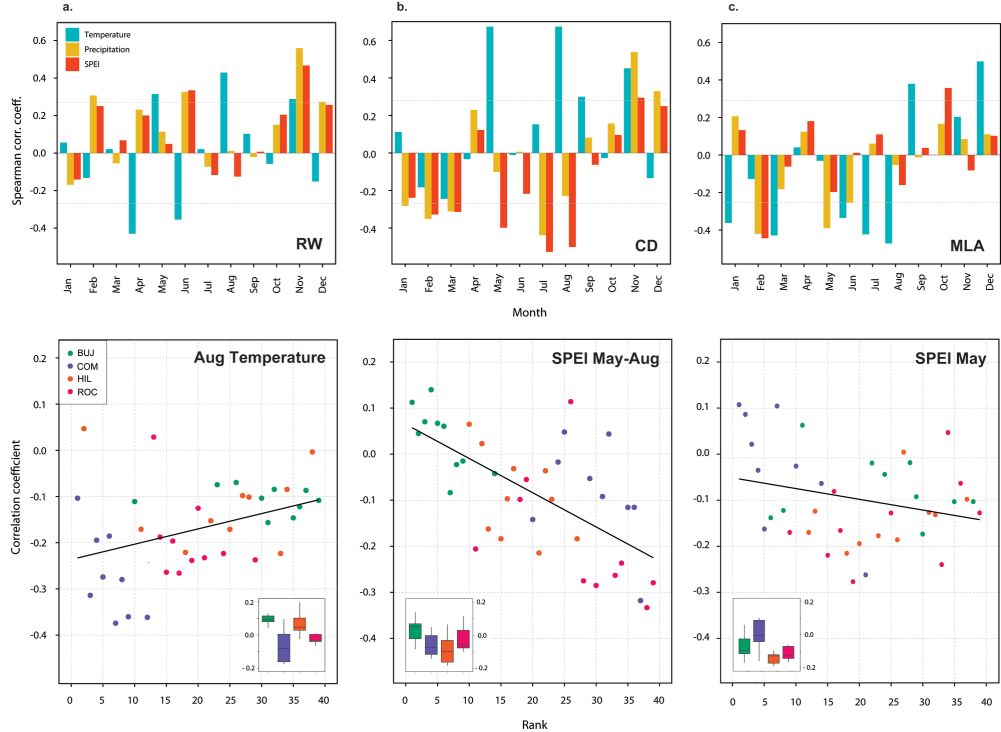
a.
b.
c.
Temperature
Precipitation
SPEI
Spearman corr. coeff.
RW
CD
MLA
Jan
Feb
Mar
Apr
May
Jun
Jul
Aug
Sep
Oct
Nov
Dec
Month
BUJ
COM
HIL
ROC
Aug Temperature
SPEI May-Aug
SPEI May
Correlation coefficient
Rank

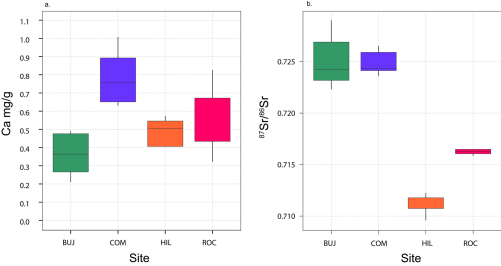
a.
Ca mg/g
1.1
1.0
0.9
0.8
0.7
0.6
0.5
0.4
0.3
0.2
0.1
0.0
BUJ
COM
HIL
ROC
Site
b.
$^{87}Sr/^{86}Sr$
0.725
0.720
0.715
0.710
BUJ
COM
HIL
ROC
Site

Site	Location (Lat, Long, wrt Limoges, region)	Characteristic of lots	Stand characteristics	Stand management
Bujaleuf (BUJ)	45.79° N, 1.63° E, 30 km E, Millevaches Regional Park.	One public-owned lot located on a south-facing slope.	Dense and narrow-spaced beech and chestnut coppice stools.	Not managed nowadays, intense past exploitation for fuel wood production.
Compreignac (COM)	45.99° N, 1.27° E, 20 km N, Ambrazac Mounts.	Valley bottom.	Oak, beech and chestnut coppice stools of varying characteristics.	Heavily exploited until 1930, regenerating ever since.
Saint-Hilaire-les-Places (HIL)	45.66° N, 1.16° E, 20 km S, Perigord-Limousin Regional Park.	Three private lots located in a flat area.	Oak and chestnut standard trees and coppice stools.	Still exploited for timber production.
Rochechouart (ROC)	45.82° N, 0.82 ° E, 30 km W, Perigord-Limousin Regional Park.	One private lot located in a flat area. Presence of wet areas.	Standard oak trees mixed with oak and chestnut coppice stools.	Absence of management for decades, charcoal production in the past

Tab. 1. Characteristics of the sampled sites

Site	BUJ	COM	HIL	ROC
Topography	On a hillside, trees from the top (430 m asl) to the bottom of a slope (405 m asl).	At mid slope (20%), all trees at the same altitude of about 370 m asl.	Trees on the top part of a gentle slope (420-425 m asl).	Trees in the middle of a gentle slope (between 265-270 m asl), not far from a wetland.
Geology	Colluvial weathered deposits. Dominant granite, very rich in biotite, almost gneissic.	Colluvial weathered deposits. Granite with 2 micas, medium grained.	All sites are very similar and positioned parallel to the front of a fault. Weathered granite with 2 micas.	Colluvial weathered deposits. Dominant granite with 2 micas.
Depth of soils	From thin (40 cm) at the top, to thick sandy loam soils (80 cm) down the slope.	Thick soils developed on a sandy granitic arena (70-80 cm).	Very thin and stony superficial soils (20 cm) to more thick ones (40-50 cm)	Very thin and stony superficial soils (20 cm).
Soil water storage capacity	From low (for thin soils with stones below 40 cm) to medium or high (for deep soils with few stones).	Relatively deep soils without stones but sandy.	Very low to low water storage capacity depending on the soil depth.	Very low (very thin soils with lot of stones below 20 cm).
Soil acidity estimation	Few plants indicative of acidic conditions, thin humus: assumption that the soil is not very acidic.	Few plants indicative of acidic conditions, thin humus: assumption that the soil is not very acidic.	Some plants indicating acidic conditions, thick humus: hypothesis of a fairly acidic soil.	Plants indicating acidic conditions and thick humus observed: hypothesis of a rather acidic soil.

Tab. 2. Description of site topography, geology and soils.

Variable	Acronym	Unit	Explanation of the variable	References
Mean cell lumen area	MLA	μm^2	Mean cell area of all measured cells in one ring	-
Maximum cell lumen area	MaxLA	μm^2	Maximum cell area of all measured cells in one ring	-
Minimum cell lumen area	MinLA	μm^2	Minimum cell area of all measured cells in one ring	-
Number of cells	CNo	No	Number of cells in one ring	-
Cumulative area of all counted cells	CTA	mm^2	Area of all counted cells in one ring	-
Mean percentage of conductive area within xylem	RCTA	%	Calculated dividing CTA by the xylem area (mm^2)	-
Cell density	CD	No/mm^2	Global mean cell density, calculated dividing the number of cells by the xylem area (mm^2)	-
Theoretical hydraulic conductivity	Kh	$m^3\ MPa^{-1}\ s^{-1}$	Accumulated potential hydraulic conductance [m^3 x s^{-1} x MPa^{-1}] as approximated by Poiseuille's law and adjusted to elliptical tubes	Tyree and Zimmermann (2002)
Theoretical xylem-specific hydraulic conductivity per annual ring	Ks	$m^2\ MPa^{-1}\ s^{-1}$	Xylem-specific potential hydraulic conductivity [m^2 x s^{-1} x MPa^{-1}] assuming a tube length of 1 m: Kh divided by xylem area (mm^2)	Tyree and Zimmermann (2002)
Mean hydraulic diameter per ring	Dh	µm	Mean hydraulic diameter per ring: [sum (2 × (cell lumen area/PI) ^0.5) ^5] / [sum (2 × (cell lumen area/PI) ^0.5) ^4]	Kolb and Sperry (1999)

Tab. 3. Vessel-related variables for which chronologies have been developed.

Chronologies	Ntrees	Parameter	EPS	Rbar	AC
Bujaleuf (BUJ)	10	TRW	0.84	0.36	0.1
		MLA	0.48	0.09	0.01
		CD	0.75	0.24	-0.03
Compreignac (COM)	9	TRW	0.89	0.5	0.324
		MLA	0.5	0.10	-0.03
		CD	0.83	0.36	0.26
Saint-Hilaire-les-Places (HIL)	10	TRW	0.82	0.33	0.04
		MLA	0.75	0.23	-0.02
		CD	0.76	0.24	0.004
Rochechouart (ROC)	10	TRW	0.86	0.4	0.17
		MLA	0.62	0.14	0.005
		CD	0.68	0.19	0.22

Tab. 4. Characteristics of the ring-width and anatomical trait chronologies.

Combining conventional tree-ring measurements with wood anatomy and strontium isotope analyses enables dendroprovenancing at the local scale

D'Andrea et al., 2022

METHODS

We combined (**1**) tree-ring width (TRW) data, (**2**) quantitative wood anatomical (QWA) measurements and (**3**) $^{87}Sr/^{86}Sr$ ratios to locate the origin of trees sampled at four sites with limited differences in climate and elevation.

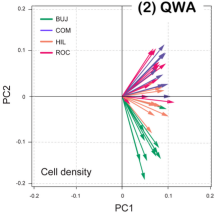

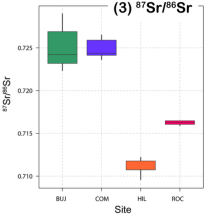

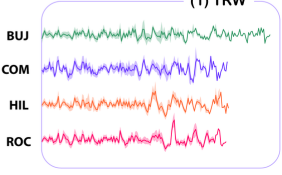

CONCLUSION

We demonstrate that the combination of xylem anatomical variables (e.g. **cell density**) with **$^{87}Sr/^{86}Sr$ ratios** allows to correctly pinpoint the origin of trees. We conclude that the multi-proxy approach adopted has the potential to increase the precision of dendroprovenancing studies at local and much larger scales.

MINISTÈRE DE LA CULTURE
Liberté
Égalité
Fraternité

LIEC

GEOLAB
Laboratoire de Géographie Physique et Environnementale

Université de Limoges